Biophysical Journal Volume 73 November 1997 2280–2291

Meta-Stability of the Hemifusion Intermediate Induced by Glycosylphosphatidylinositol-Anchored Influenza Hemagglutinin

Frank Nüssler,* Michael J. Clague,# and Andreas Herrmann*

*Humboldt-Universität zu Berlin, Mathematisch-Naturwissenschaftliche Fakultät I, Institut für Biologie/Biophysik, Berlin, Germany, and #The University of Liverpool, The Physiological Laboratory, Liverpool, UK

ABSTRACT Fusion between influenza virus and target membranes is mediated by the viral glycoprotein hemagglutinin (HA). Replacement of the transmembrane domain of HA with a glycosylphosphatidylinositol (GPI) membrane anchor allows lipid mixing but not the establishment of cytoplasmic continuity. This observation led to the proposal that the fusion mechanism passes through an intermediate stage corresponding to hemifusion between outer monolayers. We have used confocal fluorescence microscopy to study the movement of probes for specific bilayer leaflets of erythrocytes fusing with HA-expressing cells. N-Rh-PE and NBD-PC were used for specific labeling of the outer and inner membrane leaflet, respectively. In the case of GPI-HA-induced fusion, different behaviors of lipid transfer were observed, which include 1) exclusive movement of N-Rh-PE (hemifusion), 2) preferential movement of N-Rh-PE relative to NBD-PC, and 3) equal movement of both lipid analogs. The relative population of these intermediate states was dependent on the time after application of a low pH trigger for fusion. At early time points, hemifusion was more common and full redistribution of both bilayers was rare, whereas later full redistribution of both probes was frequently observed. In contrast to wild-type HA, the latter was not accompanied by mixing of the cytoplasmic marker Lucifer Yellow. We conclude that 1) the GPI-HA-mediated hemifusion intermediate is meta-stable and 2) expansion of an aqueous fusion pore requires the transmembrane and/or cytoplasmic domain of HA.

INTRODUCTION

Studies of membrane fusion mediated by spike proteins of enveloped viruses have provided a wealth of information. The influenza glycoprotein hemagglutinin (HA) is the best characterized of these proteins in terms of its structure and the properties of the fusion event it induces (for reviews see Hughson, 1995; Clague et al., 1993). Cell lines expressing HA have been widely used as model systems to characterize the nature of HA-induced fusion intermediates, using both electrical and optical techniques (Sarkar et al., 1989; Tse et al., 1993; Kemble et al., 1994). These techniques have allowed resolution of the fusion pathway into a number of defined intermediate stages, which include the establishment of a small aqueous pore, followed by the onset of lipid flow and pore dilation (Blumenthal et al., 1996; Tse et al., 1993). Mutant forms of HA have also been expressed and shown to be defective at specific intermediate stages, such, for example, that a point mutation at the amino terminus of the HA2 subunit affects only pore dilation (Schoch and Blumenthal, 1993).

Recently, it has been observed that a glycosylphosphatidylinositol (GPI)-anchored form of HA allows the flow of lipidic probes without establishing cytoplasmic continuity (Kemble et al., 1994; Melikyan et al., 1995; Nüssler et al., 1995). This latter result has been interpreted to reflect a hemifused structure that is probably very short-lived for fusion events induced by the wild-type protein (Kemble et al., 1994; Melikyan et al., 1995). The defining feature of hemifusion is the merger of the outer leaflet but not of the inner leaflet of two fusing membrane bilayers.

This hemifusion model predicts that GPI-HA will induce the redistribution of lipid probe from the outer leaflet of the target cell to the HA-expressing cell but that lipid on the inner leaflet of the target cell will remain exclusively associated with that cell, as is observed for a marker of the aqueous compartment. This has led us and others to directly test this model by developing protocols to monitor redistribution of fluorescent lipid probes that are specific for either the outer or inner bilayer leaflet of the target cell. We have developed a microscopic assay based on lipid mixing that allows simultaneous monitoring of inner-inner and outer-outer membrane leaflet fusion of WT-HA- and GPI-HA-expressing Chinese hamster ovary (CHO) cells (HA of subtype H2, X31), respectively, with human erythrocyte ghosts as a target. For that purpose, ghosts were double labeled by incorporation of the fluorescent lipids *N*-(lissamine rhodamine B sulfonyl)-dioleyl-phosphatidylethanolamine (N-Rh-PE) and 1-acyl-2-[6-[(7-nitro-2,1,3-benzoxadiazol-4-yl)amino]caproyl]-*sn*-glycero-3-phosphatidylcholine (C_6-NBD-PC) into the exoplasmic and cytoplasmic leaflets, respectively. The observed fusion behavior has been characterized in terms of NBD/Rh fluorescence intensity ratios for fused cell-ghost complexes. In contrast to WT-HA, the GPI-HA-mediated fusion exhibits a wide range of fusion behaviors from cases where both membrane leaflets merge through cases with restricted movement of inner-leaflet staining fluorescent lipids to

Received for publication 7 April 1997 and in final form 15 August 1997.

Parts of the data were presented at the American Society for Cell Biology meeting in Washington D.C. (Nüssler et al., 1995).

Address reprint requests to Dr. Andreas Herrmann, Mathematisch-Naturwissenschaftliche Fakultät I, Institut für Biologie/Biophysik, Invalidenstrasse 43, D-10115 Berlin, Germany. Tel.: 49-30-2093-8830; Fax: 49-30-2093-8585; E-mail: andreas=herrmann@rz.hu-berlin.de.

0006-3495/97/11/2280/12 $2.00

cases where only the fluorescent lipids localized at the outer leaflets mix. With time, the frequency of fusion events that display merging of the inner leaflets increases, suggesting the hemifusion intermediate as a meta-stable state. Interestingly, even after mixing of both outer and inner leaflets, we did not observe a corresponding movement of the water-soluble fluorescent dye Lucifer Yellow between erythrocytes and GPI-HA-expressing cells. This suggests an essential role of the transmembrane and/or cytoplasmic domain of HA at very late steps of the genesis of the aqueous fusion pore.

Materials and Methods

Reagents and solutions

If not otherwise indicated, chemicals were obtained from Sigma, Deisenhofen, Germany. The potassium salt of the dye Lucifer Yellow and octadecyl rhodamine B chloride (R18) were purchased from Molecular Probes, Eugene, OR, and *N*-(3-triethylammonium-propyl)-4-(6-(4-(diethylamino)-phenyl)-hexatrienyl)-pyridinium-dibromide (FM 4–64) was from Molecular Probes Europe, Leiden, Holland. 1-Palmitoyl-2-(6-(7-nitrobenz-2-oxa-1, 3-diazol-4-yl)amino)-caproyl-*sn*-glycero-3-phosphocholine (C_6-NBD-PC), 1-palmitoyl-2-(6-(7-nitrobenz-2-oxa-1, 3-diazol-4-yl)amino)-caproyl-*sn*-glycero-3-phosphoserine (C_6-NBD-PS), and the triethylammonium salt of *N*-(lissamine rhodamine B sulfonyl)-1,2-dioleyl-*sn*-glycero-3-phosphoethanolamine (N-Rh-PE) were from Avanti Polar Lipids, Alabaster, AL. Tris was from Fluka Chemie, Buchs, Switzerland. Bovine serum albumin (BSA), fraction V bovine essentially fatty acid free, was used. Phosphate-buffered saline (PBS) contained 150 mM NaCl and 5.8 mM Na_2HPO_4/NaH_2PO_4 (pH 7.4). Dulbecco's PBS (PBS+) from Biochrom, Berlin, Germany, contained 137 mM NaCl, 2.7 mM KCl, 7.3 mM Na_2HPO_4, 1.5 mM KH_2PO_4, 0.5 mM $MgCl_2$·$6H_2O$ and 0.9 mM $CaCl_2$ (pH 7.4). The hypotonic buffer contained 20 mM Hepes, 10 mM NaCl, 2 mM $CaCl_2$, and 2 mM $MgCl_2$ (pH 7.4). For ghost labeling, 100 μl of a 1 mg/ml C_6-NBD-PC or N-Rh-PE stock in chloroform was dried under nitrogen, dissolved in 15 μl of ethanol, and added to 1 ml of PBS. For labeling of CHO cells, 12 μl of C_6-NBD-PC and C_6-NBD-PS chloroform solutions (0.5 mg/ml), respectively, were dried under nitrogen and suspended in 1 ml of PBS+. To trigger fusion, ghost-cell complexes were incubated in sodium acetate buffer (NaAc buffer) containing 20 mM sodium acetate, 130 mM NaCl, 1 mM $CaCl_2$, and 1 mM $MgCl_2$ (pH 5.0).

Handling of HA-expressing CHO cells

CHO cell lines expressing stably either WT-HA (H2, X31 influenza HA) or the GPI-linked ectodomain of X31 HA (GPI-HA) were obtained from J. M. White, VA, and treated as described (Kemble et al., 1993; Kemble et al., 1994). Cells were grown in glutamine-deficient minimal essential media (G-MEM; Gibco-BRL, Life Technologies, Eggenstein, Germany) containing 10% v/v dialyzed fetal bovine serum (Gibco-BRL) and 400 mM methionine sulfoximine in a water-saturated atmosphere of 5% CO_2 in air. Before experiments, GPI-HA cells were grown in the presence of 0.25 mM deoxymannojirimycin (dMM) overnight as the latter restores the ability of GPI-HA to bind erythrocytes (Kemble et al., 1993). Cells grown to ~90% confluence were washed twice with PBS+ and for fusion experiments subsequently treated with 0.2 mg/ml neuraminidase (type V from *Clostridium perfringens*) in the presence of 5 μg/ml TPCK (*N*-Toysl-L-phenylalanine-chloromethyl ketone)-trypsin for 8 min at room temperature (limited trypsin treatment). In the majority of experiments, an additional trypsin treatment with trypsin (50 μg/ml)/EDTA (20 μg/ml) solution in PBS at 37°C for 2 min was performed (intensive trypsin treatment). Trypsinization is necessary to cleave the HA0 precursor (expressed at the membrane surface) into its fusion active subunits HA1 and HA2. After quenching trypsin by serum containing medium, cells were washed three times with PBS+.

Labeling of HA-expressing CHO cells

For control experiments, the outer and inner leaflets of HA-expressing CHO cells were labeled with C_6-NBD-PC and C_6-NBD-PS, respectively. After trypsinization, the cell suspension was centrifuged at 350 × *g* for 4 min at 4°C. The pellet (~2 × 10^6 cells) was resuspended in 100 μl of PBS+ and incubated with 300 μl of the label suspension for 20 min on ice. After one wash with PBS+, cells were incubated for another 15 min at room temperature. It is known for fibroblasts that the PS analog is rapidly transported from the exoplasmic to the cytoplasmic layer by an aminophospholipid translocase activity whereas the PC analog is not (Hanada and Pagano, 1995; Pomorski et al., 1996). In the case of C_6-NBD-PS, remaining label on the outer leaflet was subsequently removed by washing with PBS containing 2% w/v BSA. This procedure removes more than 90% of the label localized in the exoplasmic layer (data not shown). BSA was washed out with PBS+. Cells labeled on their outer leaflet with C_6-NBD-PC were washed with ice-cold PBS+ (in the absence of BSA).

Preparation of erythrocyte ghosts

Citrate-stabilized blood was obtained from the blood bank in Berlin-Lichtenberg (Berlin, Germany) or provided by the authors. After removal of the buffy coat, erythrocytes were washed twice with PBS at 2000 × *g* (10 min at 4°C). Resealed ghosts were prepared after hypotonic lysis at 4°C as described by Schwoch and Passow (1973). For preparation of N-Rh-PE/C_6-NBD-PC-labeled ghosts, a 2-ml ice-cold pellet of washed red blood cells (RBCs) was diluted in 60 ml of ice-cold lysis buffer containing 1.2 mM acetic acid, 4 mM $MgSO_4$, 1 mM $CaCl_2$, and 50 mM sodium orthovanadate. Under these conditions, the aminophospholipid translocase is blocked and lipid asymmetry cannot be maintained (Connor et al., 1990; Schrier et al., 1992; Verhoven et al., 1992). After 5 min, 1.2 mM adenosine 5′-triphosphate was added and isotonicity was established by addition of 10-fold concentrated PBS. The pH 7.4 was adjusted by 0.1 N NaOH.

Labeling of the inner leaflet of ghosts

In Fig. 1, a scheme of the procedure for double labeling of ghost membranes is shown. Before resealing, the prepared C_6-NBD-PC solution (1.67

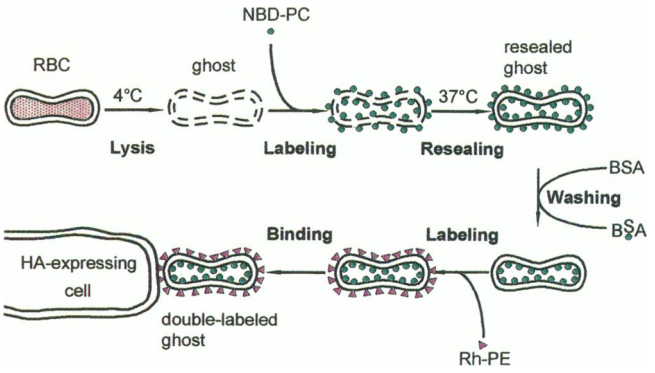

FIGURE 1 Diagram illustrating the double labeling of erythrocyte ghosts with C_6-NBD-PC and N-Rh-PE. After hypotonic lysis of human red blood cells (RBC), inner leaflet label C_6-NBD-PC is added and incorporates spontaneously into ghosts in inner and outer leaflet, respectively. After resealing of ghost membrane, BSA was added to remove C_6-NBD-PC localized at the outer membrane leaflet. Finally, inner leaflet labeled resealed ghosts were incubated with N-Rh-PE, which inserts only in the outer leaflet of ghost membranes (for details see Materials and Methods).

μg/ml final concentration; see Reagents and solutions) was added to the ghost suspension under rapid stirring. Ghosts were resealed by incubation at 37°C for 45 min and collected by centrifugation at 13,000 rpm (8 min at 4°C). Then, ghosts were washed twice with PBS. Subsequently, C_6-NBD-PC located in the outer leaflet was removed by two washing steps with PBS containing 2% w/v BSA. Finally, the ghost suspension was washed once with PBS.

For preparing ghosts double labeled with FM4-64 and C_6-NBD-PC, we performed hypotonic lysis (see above) and FM 4-64 (1 mg/ml) was incorporated as described for Lucifer Yellow. Subsequently, C_6-NBD-PC was incorporated as described above.

Labeling of the outer leaflet of ghosts

N-Rh-PE was incorporated in the outer leaflet of ghosts by addition of the prepared label solution (see Reagents and solutions) to the pellet followed by a 2-min incubation at 37°C (Fig. 1). Afterward, ghosts were spun down and washed once with ice-cold PBS. These double-labeled ghosts were stored on ice until use for no longer than 6 h.

Preparation of Lucifer Yellow-filled ghosts co-labeled with N-Rh-PE or C_6-NBD-PC

Ghost preparation and labeling with N-Rh-PE were carried out as described above with the following modifications. After lysis, the pellet was resuspended in 5 ml of the lysis buffer containing 1 mg/ml Lucifer Yellow and incubated for 5 min at 4°C. For C_6-NBD-PC labeling, the prepared stock of the dye (see above; 90 μg total) was added at this time. Ghosts were resealed at 37°C after adjusting to isotonic conditions and pH 7.4. Subsequently, ghosts were washed three times with PBS to remove unincorporated Lucifer Yellow.

Dithionite assay

To assess the transbilayer orientation of C_6-NBD-analogs in the plasma membrane of ghosts and of HA-expressing CHO cells, we used the dithionite assay as described by McIntyre and Sleight (1991) with modifications of Pomorski et al. (1994). Chemical reaction of the NBD group with dithionite causes an irreversible loss of its fluorescence properties (McIntyre and Sleight, 1991). We have shown that at low temperature dithionite rapidly reduces only C_6-NBD-PC localized on the exoplasmic but not on the inner leaflet of mammalian plasma membranes (Pomorski et al., 1994, 1996). Briefly, a 20-μl pellet of labeled ghosts, CHO cells, or cell-ghost complexes was diluted in 2 ml of PBS (4°C at pH 7.4) in a fluorescence cuvette. The final concentrations were $\sim 5 \times 10^7$ ghosts/ml and $\sim 7 \times 10^6$ CHO cells/ml in the two latter cases. The time trace of NBD fluorescence (λ_{ex} = 470 nm; λ_{em} = 540 nm) was recorded at 4°C using an Aminco Bowman Series-2 spectrofluorimeter (SLM Aminco Instruments, Urbana, IL). After 30 s, dithionite from a freshly prepared stock (1 M dithionite in PBS containing 100 mM TRIS) was added to a final concentration of 50 mM. For 100% label reduction, Triton X-100 was added to a final concentration of 0.5% at the end of each time trace.

Back-exchange assay

The amount of C_6-NBD phospholipid analogs on the outer leaflet of the plasma membrane was assessed by the back-exchange of those analogs to BSA at pH 7.4. For control measurements, a 20-ml pellet of labeled ghosts ($\sim 10^8$ ghosts) was gently vortexed with BSA (3.3% final concentration) and incubated on ice for 1 min. In the case of CHO cell-ghost complexes, the back-exchange was done in the same way but with 50 ml of CHO cell-ghost suspension ($\sim 3 \times 10^6$ cells). Fusion between HA-expressing CHO cells and ghosts labeled on the inner leaflet was performed as described for double-labeled ghosts (see below). Cell-ghost complexes or ghosts were spun down by a short centrifugation (40 s at 7000 × *g*). Supernatants and pellets were separated and NBD fluorescence was measured. The sum of the fluorescence of the pellet and that of the supernatant for each sample was taken as 100%.

Estimation of degree of trypsinization of HA on CHO cells

Samples from WT-HA-expressing cells were treated with the two different trypsin concentrations described above. Western blotting was done using rabbit polyclonal antibodies (gift from J. Skehel). Visualization of HA0 was achieved using enhanced chemiluminescence.

Microscopic studies

HA-expressing CHO cells on a chambered coverglass (Nunc, Naperville, IL) were incubated with 2 ml of a 0.2% suspension of double-labeled ghosts in the dark for 15 to 20 min on ice. Unbound ghosts were removed by five to seven washes with PBS+. Fusion was induced by a 2-min incubation of the cell-ghost complexes with NaAc buffer, pH 5.0, at 37°C. The acidic buffer was replaced by PBS (37°C), and cell-ghost complexes were observed for up to 40 min at room temperature by a confocal laser scanning microscope (Noran Instruments, Middleton, WI) with a 40× oil immersion objective (Nikon, Tokyo, Japan). During this period, images were digitally stored by using the software Intervision 1.1 (Noran Instruments) and arranged by time (minutes). The time delay between the storage of the rhodamine and the NBD fluorescence, respectively, for one single image was in the range of a few seconds.

Analysis of Rh/NBD fluorescence micrographs

After background subtraction, fluorescence images were analyzed by eye to count the number of fused cell-ghost complexes. The fusion events in the case of GPI-HA were divided into three classes of membrane fusion behavior: 1) full membrane fusion (FMF), 2) restricted fusion (RF), and 3) hemifusion (HF).

Fusion events were quantitatively analyzed by selecting regions of interest, which means the area of a CHO cell or a ghost, respectively, using the public domain program NIH Image 1.57 (developed at the U.S. National Institutes of Health and available from the Internet by anonymous FTP from zippy.nimh.nih.gov or on floppy disk from the National Technical Information Service, Springfield, VA, part PB95-500195GEI) running on a Power Macintosh 6100/66. From the regions of interest, the mean intensity of the Rh and of the NBD fluorescence, respectively, was calculated for all selected pixels. To compare ghosts and cells (wild type and mutant), the ratio of the mean NBD fluorescence intensity to the mean Rh fluorescence intensity (NBD/Rh ratio) was calculated for single ghosts as well as cells.

RESULTS

We have divided this section in two parts. In the first part, fusion mediated by WT-HA and GPI-HA is compared. In the second part, the relevant control experiments that have been used to validate the assay for inner leaflet mixing are presented.

WT-HA- and GPI-HA-mediated fusion

Monitoring of membrane fusion and formation of an aqueous fusion pore

The fusion activity of the WT-HA- and GPI-HA-expressing CHO cells was probed at 37°C by the well established R18

fluorescence dequenching (FDQ) assay between R18-labeled RBCs and HA-expressing CHO cells (Hoekstra et al., 1984; Morris et al., 1989). In agreement with previous results (Kemble et al., 1994; Melikyan et al., 1995), efficient lipid mixing as reflected by FDQ occurred after addition of HA-expressing CHO-RBC complexes to acidic NaAc buffer (pH 5.0) at 37°C (data not shown). Reneutralization after 180 s of incubation at low pH did not inhibit subsequent FDQ and, thus, lipid mixing (see also Morris et al., 1989). The kinetics and the extent of FDQ were similar for WT-HA- and GPI-HA-mediated fusion for the fusion optimal conditions probed.

Membrane merger as well as the formation of an aqueous fusion pore between fusing cells and ghosts were examined in parallel by fluorescence microscopy. Ghosts were double labeled with N-Rh-PE incorporated into the outer leaflet and the water-soluble dye Lucifer Yellow ($M_r \approx 500$). Fusion of the exoplasmic leaflet between ghosts and CHO cells visible by the redistribution of N-Rh-PE from ghosts to HA-expressing cells was observed for both WT-HA and GPI-HA. Labeling of the cytoplasm of HA-expressing cells by Lucifer Yellow after triggering fusion is indicative of the formation of an aqueous fusion pore. This was observed in the case of WT-HA but not for GPI-HA (Fig. 2), which is in agreement with previous observations (Kemble et al., 1994; Melikyan et al., 1995). After a short (~30 s) exchange of isoosmotic (~300 mosmol/L) PBS for hypotonic buffer (see Materials and Methods), we observed in some cases the spread of Lucifer Yellow to CHO cells for GPI-HA-mediated fusion (Fig. 2 *C* and *F*) as also observed by Melikyan et al. (1995). For GPI-HA-mediated fusion examined using C_6-NBD-PC/Lucifer Yellow-labeled ghosts we found ~2% of C_6-NBD-PC-stained cells also stained with Lucifer Yellow. These results show that labeling of the inner and outer leaflets by C_6-NBD-PC and N-Rh-PE, respectively, does not significantly affect aqueous content mixing, either in the case of WT-HA or in the case of GPI-HA.

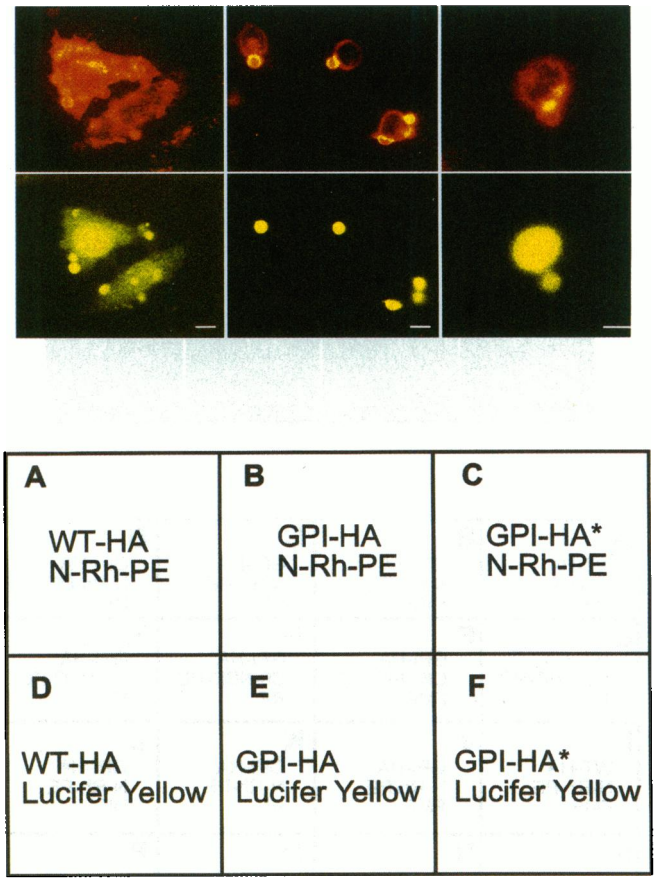

FIGURE 2 Fluorescence micrographs visualizing lipid (N-Rh-PE; *upper panel, A, B, and C*) and content (Lucifer Yellow; *lower panel, D, E,* and *F*) mixing between WT-HA-expressing (*left panel, A* and *D*) and GPI-HA-expressing (*middle* and *right panels, B, C, E, and F*) and cells and ghosts double labeled with Lucifer Yellow and N-Rh-PE (outer membrane leaflet). Cells expressing WT-HA or GPI-HA were treated with neuraminidase/trypsin (200 mg/5 mg per ml) for 8 min at room temperature and in addition with trypsin (50 mg/ml)/EDTA (20 mg/ml) solution in PBS at 37°C for 2 min. After quenching with medium, double-labeled ghosts (0.2% suspension) were bound (15 min at 4°C). Subsequent to a 2-min incubation in NaAc buffer (pH 5.0 at 37°C), the cell-ghost complexes were returned to neutral pH buffer (PBS+) at room temperature and then observed and photographed within 45 min. In the right panel (*C* and *F*), one GPI-HA-expressing cell-ghost complex is shown after PBS+ was exchanged by hypotonic buffer (~72 mosmol/L) for ~30 s. Bar, 10 μm.

Monitoring of inner-inner and outer-outer membrane leaflet fusion (NBD/Rh leaflet assay)

Upon triggering fusion by acidification (pH 5.0), we followed the redistribution of lipid analogs that had been selectively incorporated into the outer (N-Rh-PE) and inner leaflet (C_6-NBD-PC) of ghost membranes. For WT-HA-mediated fusion, we found that the fluorescence intensity of N-Rh-PE as well as of C_6-NBD-PC associated with fused CHO cells was similar to the donor ghost membranes. This indicates a complete lipid redistribution for both the outer and inner bilayer leaflets. We refer to this type of membrane fusion behavior as full membrane fusion (Fig. 3, *A, E, I,* and *M*). Please note that full membrane fusion here is synonymous for both inner and outer leaflet fusion but does not essentially include cytoplasmic continuity. There were less than 2% of fused cell-ghost complexes per experiment showing a less intense NBD fluorescence of WT-HA-expressing CHO cells in comparison with ghost(s), which we categorize as restricted fusion behavior. A typical feature of WT-HA-mediated fusion was the intense staining of cytoplasmic compartments of the fused CHO cells by C_6-NBD-PC (compare Fig. 3). This is strong evidence that the PC analog is oriented toward the cytosolic leaflet (Pomorski et al., 1996) even after fusion (see also below). Indeed, as verified by fluorescence microscopy, the NBD fluorescence of fused cell-ghost complexes was not affected by addition of BSA (~3% final concentration, not shown). In control experiments we have shown that this procedure causes a complete loss of the NBD fluorescence of both ghosts and CHO cells, provided that C_6-NBD-PC was localized in the exoplasmic leaflet. Neither for WT-HA nor for GPI-HA-

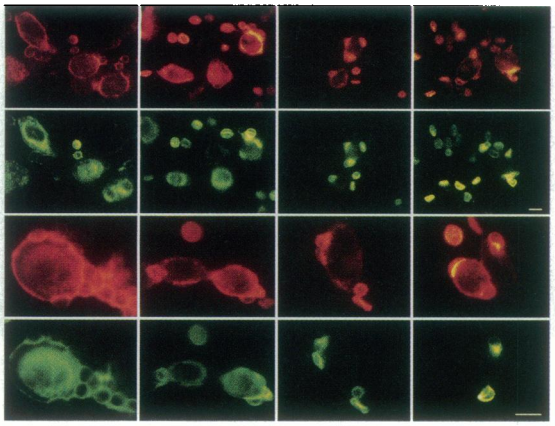

A WT-HA N-Rh-PE FMF	**B** GPI-HA N-Rh-PE FMF	**C** GPI-HA N-Rh-PE RF	**D** GPI-HA N-Rh-PE HF
E WT-HA C6-NBD-PC FMF	**F** GPI-HA C6-NBD-PC FMF	**G** GPI-HA C6-NBD-PC RF	**H** GPI-HA C6-NBD-PC HF
I WT-HA N-Rh-PE FMF	**J** GPI-HA N-Rh-PE FMF	**K** GPI-HA N-Rh-PE RF	**L** GPI-HA N-Rh-PE HF
M WT-HA C6-NBD-PC FMF	**N** GPI-HA C6-NBD-PC FMF	**O** GPI-HA C6-NBD-PC RF	**P** GPI-HA C6-NBD-PC HF

FIGURE 3 Inner and outer membrane leaflet mixing between ghosts and HA-expressing cells as detected by using N-Rh-PE/C_6-NBD-PC-labeled ghosts. Preincubation of WT-HA-expressing (*left panel, A, E, I,* and *M*) and GPI-HA-expressing cells and subsequent binding of double-labeled ghosts and pH 5 fusion trigger were performed as described in the legend of Fig. 2. In the case of GPI-HA, we distinguished three classes of fusion behavior by analyzing the effectiveness of label redistribution between appropriate fusion partners: 1) N-Rh-PE (outer leaflet) redistribution only (hemifusion, HF; *D, H, L,* and *P*), 2) N-Rh-PE redistribution and partial redistribution of inner leaflet label C_6-NBD-PC (restricted fusion, RF; *C, G, K,* and *O*), and 3) both labels (outer and inner leaflet lipids) equilibrated between ghost and cell membranes (full membrane fusion, FMF; *B, F, J,* and *N*). In the case of WT-HA, only the latter is observed (FMF; *A, E, I,* and *M*). Rh (*A–D* and *I–L*) and NBD (*E–H* and *M–P*) fluorescence are shown. Bar, 10 μm (images in lower two panels are zoomed twice). For additional details, see text and Materials and Methods.

mediated membrane fusion could we detect any Rh fluorescence of the cytoplasm of fused complexes, consistent with the exclusive localization of N-Rh-PE on the outer leaflets.

For GPI-HA cells, we found a broad distribution of membrane fusion behaviors as deduced from the distribution of C_6-NBD-PC fluorescence between fused CHO cells and ghosts. Besides full membrane fusion (see above), we found a significant percentage of fusion that we classified as restricted (Fig. 3 *C, G, K,* and *O*; see also above) as well as the expected hemifusion. The latter is characterized by a redistribution of N-Rh-PE but no movement of C_6-NBD-PC to GPI-HA-expressing cells after triggering fusion (Fig. 3 *D, H, L,* and *P*). In Fig. 4, the relative contribution of each fusion class to all fusion events counted is shown for WT-HA- and for GPI-HA-mediated membrane fusion observed over a time period of 44 min after triggering fusion by low pH and subsequent reneutralization. For a detailed analysis of the time dependence, see below. We have also compared the influence of limited and intensive pretreament of HA-expressing cells with trypsin (see Materials and Methods) on the relative frequency of the different fusion events (Fig. 4, *A* and *B*). In both cases of pretreatment we found that, for WT-HA, full membrane fusion dominated, whereas for GPI-HA, restricted fusion and hemifusion were also common. There was no significant influence of the different trypsin pretreatments on the WT-HA-mediated fusion, but in the case of GPI-HA, the frequency of the three different fusion classes (full membrane, restricted, and hemifusion) was significantly changed (Fig. 4). After limited trypsin

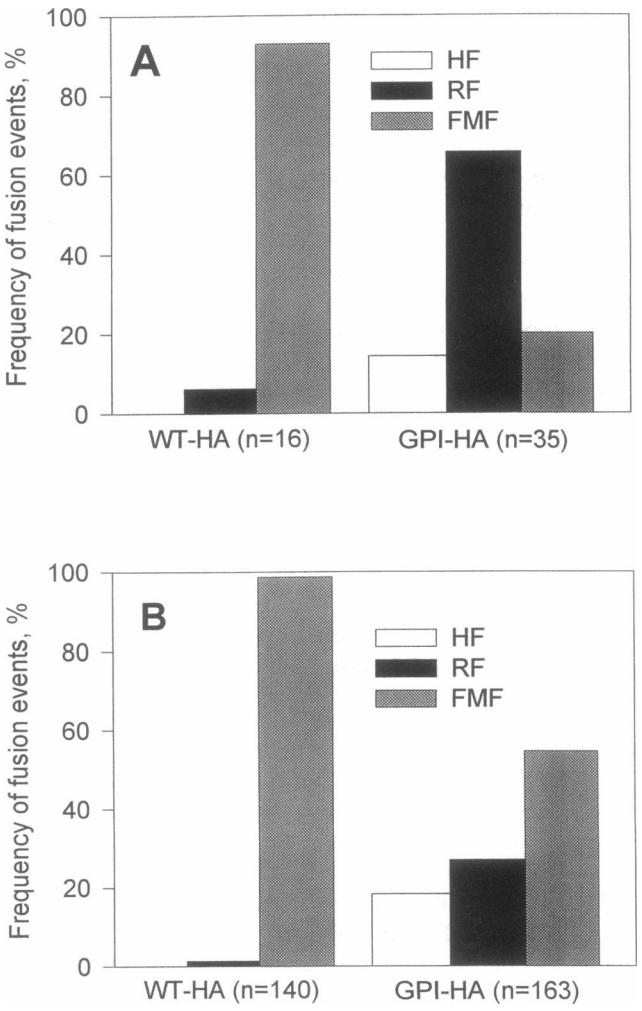

FIGURE 4 Comparison of limited (*A*) and intensive (*B*) trypsin pretreatment of WT-HA and GPI-HA, respectively, and its influence on the frequency of fusion events with respect to the observed classes of fusion behavior: hemifusion (HF), restricted fusion (RF), and full membrane fusion (FMF) (see text for details).

pretreatment, the restricted fusion was prevalent (~60%) compared with full and hemifusion (~20% each). In contrast, after intensive trypsin treatment, full membrane fusion was clearly favored (~60%), whereas restricted fusion was significantly reduced. Hemifusion was not affected by intensive trypsin pretreatment. We note that the total number of fusion events is increased after intensive trypsin treatment. This suggests that the concentration of cleaved HA0 by trypsin affects the number of fusion events (WT-HA and GPI-HA) as well as the extent of full membrane fusion (GPI-HA). Using immunoblotting of HA, we estimated approximately 60% HA0 cleavage after limited trypsin treatment of WT-HA-expressing cells when compared with the same cells after intensive trypsin treatment (data not shown).

For a quantitative verification of the observed fusion behavior, in particular, the appearance of two distinct fusion classes (hemifusion and full membrane fusion) and an intermediate state (restricted fusion) in the case of GPI-anchored HA, the ratio of the mean NBD fluorescence density to the mean Rh fluorescence density (NBD/Rh ratio) was calculated for fused CHO cells as well as for fused ghosts. For comparison, we determined also the NBD/Rh ratio of unfused ghosts. For the following data analysis, experiments with intensive trypsin pretreatment of HA-expressing cells were chosen to ensure a higher number of fusion events during the experimental time course.

Between different ghost preparations we found a significant variation in the NBD/Rh ratio of unfused ghosts. In Table 1 we have compared the fluorescence ratio of ghosts from three different preparations. As can be seen, the ratio varied up to a factor of 3 (comparison of experiments 1 and 3). As judged from emission spectra of freshly prepared ghosts and image analysis, the variation of the ratio was mainly ascribed to differences of the N-Rh-PE fluorescence whereas the NBD intensity was almost constant between independent experiments. We do not know the precise reason for the variability in N-Rh-PE labeling. It is important to note that the variation of the average NBD/Rh-ratio is not due to extreme scattering of values. The standard error of estimate is in all cases on the order of 6 to 9% of the average (Table 1).

In Table 1 we have compared for different preparations the NBD/Rh ratio of unfused ghosts with that of ghosts and of CHO cells that have undergone full fusion. As expected, an enhanced NBD/Rh ratio of unfused ghosts (before fusion) is always accompanied by an increase of that ratio for the respective fused ghosts and CHO cells.

We found that the mean NBD/Rh ratio of unfused ghosts was in all experiments greater than that of ghosts that have undergone full membrane fusion either by WT-HA or by GPI-HA (Table 1). This is not caused by extreme values. The whole distribution of the NBD/Rh ratio of unfused ghosts is shifted relative to that of fused ghosts (Figs. 5 and 6 *E*). This may be due to 1) a (partial) release of fluorescence quenching by N-Rh-PE after redistribution between the outer leaflets of CHO and ghost plasma membranes (we found that N-Rh-PE incorporated into ghost membranes becomes significantly quenched even at low probe concentration; data not shown) or 2) redistribution of C_6-NBD-PC toward subcellular membranes of CHO cells causing a depletion of the fused inner leaflets on that analog and, in parallel, an enrichment of the analog in the cytoplasm of CHO cells. Even in the presence of an aqueous fusion pore (in the case of WT-HA), such an enrichment is probable as a significant movement of CHO organelles to the lumen of ghosts was not observed.

In Fig. 6 we have compared the distribution of the NBD/Rh ratio of full fusion (*A* and *E*, WT-HA; *B* and *F*, GPI-HA), of GPI-HA-mediated restricted fusion (*C* and *G*), and hemifusion (*D* and *H*) for fused CHO cells (*A–D*) and fused ghosts (*E–H*) of a typical experiment. As expected, for fused CHO cells we found the following sequence for the NBD/Rh ratio: $[NBD/Rh]_{FMF,\ WT} \approx [NBD/Rh]_{FMF,\ GPI} > [NBD/Rh]_{RF,\ GPI} > [NBD/Rh]_{HF,\ GPI}$. Likewise, we found a sequence of the average fluorescence ratio for fused ghosts that is the reverse of that of CHO cells: [NBD/

TABLE 1 Mean NBD/Rh ratios for different preparations

	NBD/Rh ratio (average ± SEM)		
Preparation	Unfused ghosts	Fused ghosts (WT-HA, FMF)	Fused cells (WT-HA, FMF)
1	1.10 ± 0.10 (n = 21)	0.48 ± 0.06 (n = 21)	1.35 ± 0.06 (n = 52)
2	2.62 ± 0.14 (n = 58)	0.75 ± 0.05 (n = 40)	2.55 ± 0.13 (n = 34)
3	3.68 ± 0.22 (n = 39)	1.34 ± 0.18 (n = 14)	3.22 ± 0.35 (n = 13)

Variation of the NBD/Rh density ratio of three independent ghost preparations. Data are shown for unfused ghosts as well as for ghosts and WT-HA-expressing CHO cells that have undergone full membrane fusion (FMF) mediated by WT-HA. The average ratio and SEM are given (n = number of ghosts/CHO cells counted).

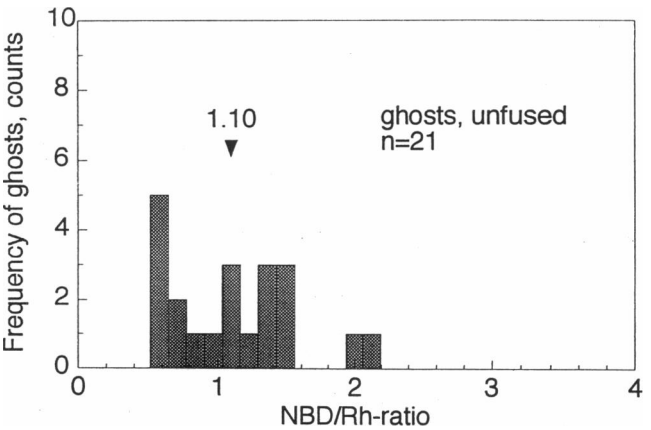

FIGURE 5 NBD/Rh ratio distribution calculated from unfused ghosts. The mean value is indicated by an arrowhead. Data were obtained from one typical experiment with the indicated numbers of measured ghosts (bin size, 0.13; 31 bins).

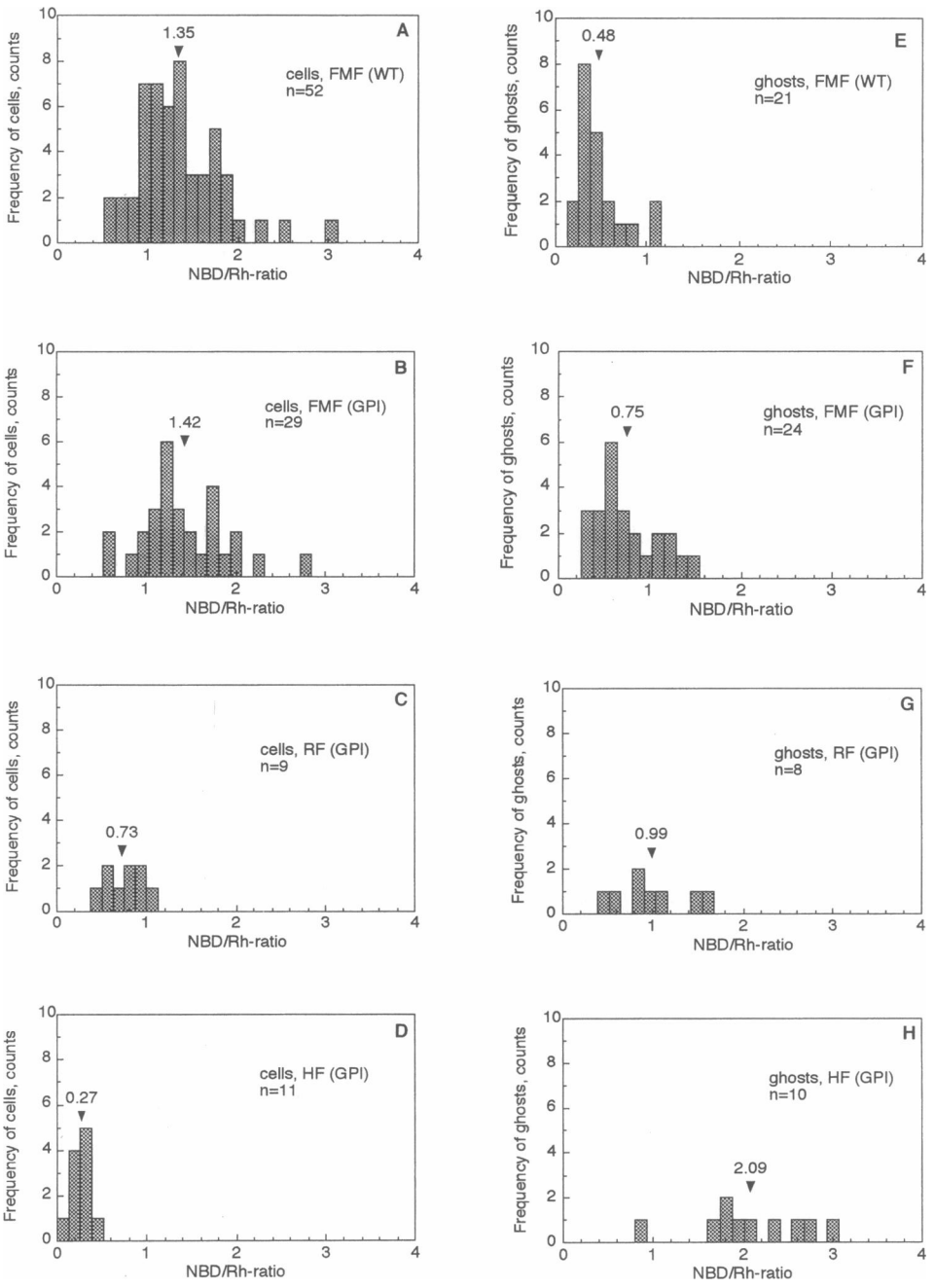

FIGURE 6 NBD/Rh density ratio distribution calculated from CHO cells and ghosts, respectively, that have undergone full membrane fusion (FMF), restricted fusion (RF), and hemifusion (HF). For definitions, see Fig. 3. Mean values of ratios are indicated by arrowheads. Data were obtained from one typical experiment with the indicated numbers of measured cells and ghosts, respectively (bin size, 0.13; 31 bins).

$Rh]_{FMF,\ WT} < [NBD/Rh]_{FMF,\ GPI} < [NBD/Rh]_{RF,\ GPI} < [NBD/Rh]_{HF,\ GPI}$. The change of the average ratio is paralleled by a shift of the distribution as well as its maximal and minimal values. The maximal standard error of estimate is 11 and 13% of the average ratio for cells and ghosts, respectively. Whereas for CHO cells the fluorescence ratio for full fusion is similar for WT-HA and GPI-HA, we found an enhanced ratio for ghosts that have undergone GPI-HA-mediated full membrane fusion relative to those ghosts fully fused with WT-HA-expressing cells.

So far we have summarized and analyzed fusion events independently of the time of their observation after triggering fusion. We have also analyzed the frequency of fusion events as a function of time with a resolution of 8 min. For that purpose three independent experiments were counted. The time dependence of the relative frequency of all fusion events is similar for WT-HA (full membrane fusion) and GPI-HA (full, restricted, and hemifusion). After a time of >8 min of triggering fusion, the WT-HA-mediated fusion reached a plateau (not shown). Although the same conclusion can be drawn for GPI-HA-mediated fusion, significant changes of the relative contribution of different fusion classes occurred for times >8 min. In Fig. 7 the distribution of fusion events between full, restricted, and hemifusion is shown as a function of time. In this graph the sum of all fusion events for each time point (8, 16, etc. min) was set to

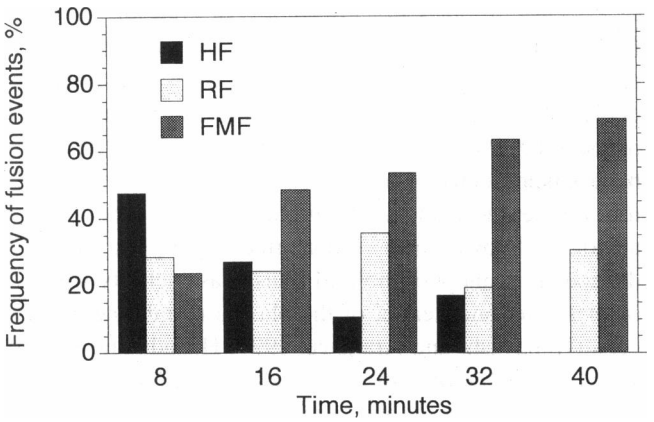

FIGURE 7 The frequency of the distinguished three classes of fusion behavior of GPI-HA-mediated fusion (see also Fig. 3) as a function of time. Time scale was divided into five classes (bin size, 8 min). HF, hemifusion; RF, restricted fusion; FMF, full membrane fusion.

100%. In the early phase subsequent to a fusion trigger, most frequently hemifusion was found. Later on, after ~16 min, the number of hemifusion events was decreased as the number of full membrane fusion events increased. The relative frequency of restricted fusion was almost constant. For times longer than >32 min after lowering pH, no HF event was detected (Fig. 7).

Monitoring of inner-inner leaflet fusion simultaneously by C_6-NBD-PC and FM 4–64

Recently, Melikyan et al. (1995) employed the fluorescence probe FM 4–64 to follow inner leaflet fusion between HA-expressing CHO cells and human erythrocyte ghosts. FM 4–64 is a nonpermeable double-charged, cationic probe that becomes strongly fluorescent upon partition into the membrane. Incorporation of FM 4–64 into the inner leaflet of ghosts is performed by a procedure similar to what we have used for Lucifer Yellow. In contrast to our results with C_6-NBD-PC, Melikyan et al. (1995) did not observe any labeling of CHO cells by FM 4–64 upon GPI-HA-mediated membrane fusion, whereas strong labeling was detected in the case of WT-HA. To see whether both membrane probes exhibit a different behavior of redistribution between ghosts and HA-expressing cells after triggering fusion, we co-labeled ghosts with C_6-NBD-PC and FM 4–64 at the inner leaflet. First, we studied WT-HA-mediated fusion, which was characterized by a strong staining of the plasma membrane and cytoplasm of CHO cells by both labels (Fig. 8). Bright FM 4–64 spots were observed, presumably due to an accumulation of the probe in organelles of CHO cells. Although less intense, the NBD fluorescence was clearly visible in the CHO cell cytoplasm (Fig. 8). Next, we examined the redistribution of both probes in the case of GPI-HA-mediated membrane fusion. Because we labeled only the inner leaflet of ghosts, we distinguished only between restricted and full fusion. Approximately 65% of GPI-HA-

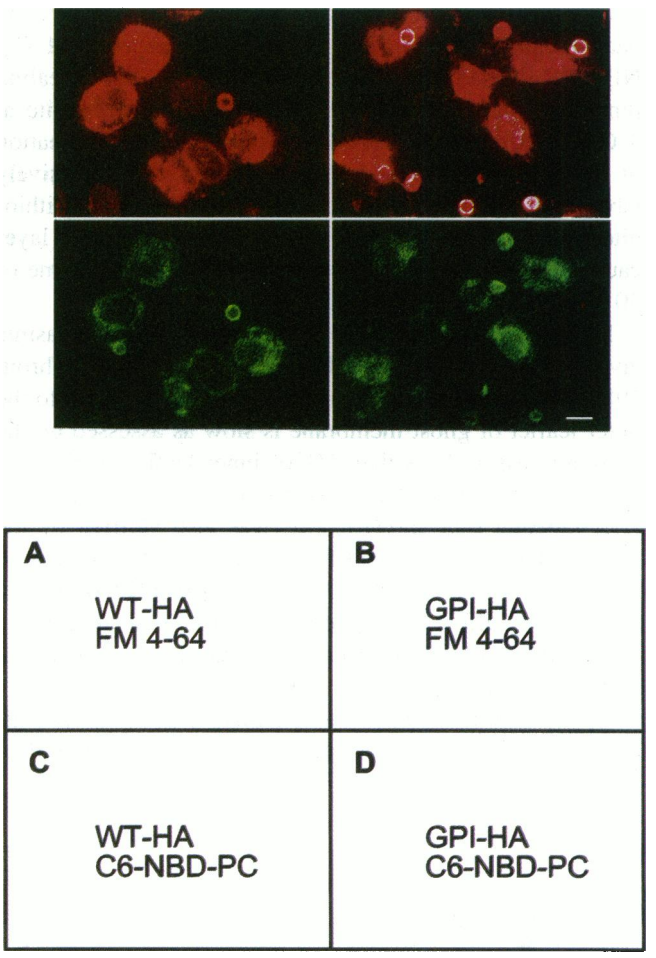

FIGURE 8 Fluorescence micrographs of WT-HA-mediated (*left panel, A* and *C*) and GPI-HA-mediated (*right panel, B* and *D*) fusion between HA-expressing cells and ghosts initially loaded with FM 4–64 (*upper panel, A* and *B*) and inner membrane leaflet labeled with C_6-NBD-PC (*lower panel, C* and *D*). For labeling procedure see Materials and Methods. Preincubation and fusion trigger were as described in Fig. 2. Bar, 10 μm.

expressing cells that have undergone membrane fusion (n = 37) clearly showed an intense labeling by both dyes indicating full membrane fusion of both plasma membranes. Thus we observed also by FM 4–64 a fusion of the inner leaflets with GPI-HA-expressing cells. For ~35% of observed fusion events we found a restricted redistribution of dyes to CHO cells. In more than one-half of those cases we found a similar restricted redistribution of both dyes, whereas in other cases the degree of redistribution was different.

Assay for simultaneous monitoring of inner-inner and outer-outer leaflet merger

Stability of the transbilayer orientation of fluorescent lipid analogs in ghosts and CHO cells

The outer and inner leaflets of human erythrocyte ghost membranes were labeled with N-Rh-PE and C_6-NBD-PC, respectively. An important step in preparation of those

double-labeled ghosts was the removal of C_6-NBD-PC by back-exchange to BSA. Indeed, the fluorescence of C_6-NBD-PC-labeled ghosts washed with BSA after resealing remained almost constant in the presence of dithionite at 4°C (Fig. 9, curve A). This demonstrates that 1) permeation of dithionite is slow and 2) those ghosts are exclusively labeled on the inner leaflet. In contrast, addition of dithionite to ghosts labeled only on the outer membrane layer caused a fast loss of total fluorescence with a half-time of 30 s (n = 2; Fig. 9, curve E).

N-Rh-PE is known to reside stably in the exoplasmic layer of erythrocyte membranes (Connor and Schroit, 1987). The movement of C_6-NBD-PC from the inner to the outer leaflet of ghost membrane is slow as assessed by the dithionite assay. Less than 5% of inner leaflet label redistributed to the outer leaflet when stored on ice for 1 day after labeling (not shown). This was also verified by the back-exchange of label to BSA (6% of analog accessible to BSA). Importantly, incubation at acidic pH (pH 5.0) did not significantly affect the movement of the PC analog to the ghost outer leaflet (8% accessible) in comparison with that at pH 7.4.

To measure unambiguously the merger of the inner leaflets of fusing membranes requires that the orientation of

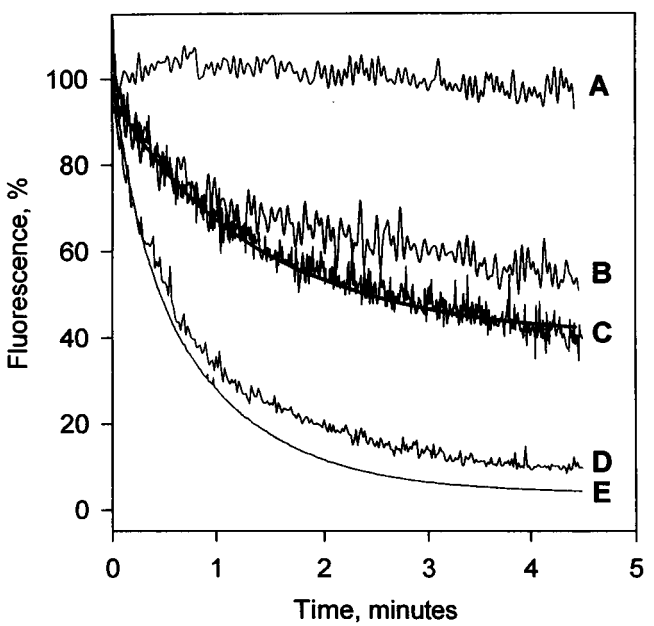

FIGURE 9 Quenching of the fluorescence of NBD-labeled phospholipid analogs by dithionite in PBS at pH 7.4 and 4°C. (*A*) Cell-ghost complexes after a brief incubation at pH 7.4 and 37°C (control), with inner membrane leaflet of ghosts labeled with C_6-NBD-PC; (*B*) WT-HA-expressing CHO cells after a brief incubation at pH 5.0 and 37°C, with inner leaflet labeled with C_6-NBD-PS; (*C*) Cell-ghost complexes after fusion (3-min incubation at pH 5.0 and 37°C), with inner leaflet of ghosts initially labeled with C_6-NBD-PC; (*D*) WT-HA-expressing cells after a 3-min incubation at pH 5.0 and 37°C, with outer leaflet labeled with C_6-NBD-PC; (*E*) ghosts, with outer leaflet labeled with C_6-NBD-PC. Dithionite (100 mM final concentration) was added at time 0. For details see Materials and Methods as well as Results.

C_6-NBD-PC to the cytosolic leaflets of both plasma membranes remains unaffected by the fusion process. We first characterized dithionite quenching of C_6-NBD-labeled phospholipid analogs in the plasma membrane of HA-expressing CHO cells. For labeling of the cytosolic leaflet, we have labeled cells with C_6-NBD-PS and incubated for 20 min on ice and another 15 min at room temperature. This analog is known to be transported rapidly by an ATP-dependent aminophospholipid translocase activity from the outer to the inner leaflet of the plasma membrane of CHO cells (Kobayashi and Arakawa, 1991; Hanada and Pagano, 1995). After removal of the remaining C_6-NBD-PS in the exoplasmic leaflet by back-exchange to BSA, HA-expressing CHO cells were incubated for 3 minutes at pH 5.0 (37°C). Subsequently, the fluorescence was measured at pH 7.4 at 4°C in the presence of dithionite. As can be seen (Fig. 9, curve B) in contrast to erythrocyte ghosts, a continuous fluorescence decrease was found that could be described by a monoexponential function with a half-time ($t_{1/2}$) of 57.1 ± 2.1 sec (n = 3). We ascribe the decrease of the fluorescence intensity of C_6-NBD-PS to a rather high permeability of the CHO plasma membrane to dithionite even at low temperature but not to unremoved analogs in the outer leaflet for the following reasons. First, repeated washing of cells with BSA did not reduce or even abolish the fluorescence loss. Second, we did not observe a rapid initial fluorescence decrease upon addition of dithionite (data not shown). We would expect to see this for C_6-NBD analogs localized in the outer leaflet. Indeed, we found a fast drop ($t_{1/2}$ = 30 s) of the fluorescence (pH 7.4 at 4°C) similar for both analogs, C_6-NBD-PC and C_6-NBD-PS, when dithionite was added immediately after labeling of HA-expressing cells on ice (not shown). A similar rapid decline of fluorescence ($t_{1/2}$ = 28.1 ± 0.2 s; n = 3) was observed after a short preincubation at pH 5.0 for 3 min (Fig. 9, curve D). In those cases, all analogs are confined almost exclusively to the exoplasmic leaflet verified by the complete removal of the analog by washing cells with BSA.

Addition of dithionite to cell-ghost complexes after triggering fusion causes a loss in fluorescence intensity (Fig. 9, curve C) that can be well fitted by a monoexponential function ($t_{1/2}$ = 64.8 ± 3.8 s; n = 3). The kinetics are almost identical to that obtained in the case of HA-expressing cells labeled with C_6-NBD-PS on the cytosolic face ($t_{1/2} \approx$ 57 s; see above). Again, this is a strong indication that the fluorescent PC analog is still oriented to the inner leaflet. This is supported by the back-exchange assay (see also above). Although we found a slight increase of the amount of C_6-NBD-PC extractable by BSA for fused CHO cell-ghost complexes in comparison with ghosts alone, it is obvious that the fusion event did not cause a remarkable increase of this amount (increase of 4% of accessible analog). In conclusion, the data clearly show that the transmembrane orientation of C_6-NBD-PC is not altered by the fusion process.

DISCUSSION

In the present study we have used fluorescent phospholipid analogs to specifically label the inner and outer leaflets of resealed erythrocyte ghosts. This has allowed us to compare the redistribution of each monolayer independently after membrane fusion with CHO cells expressing either WT-HA or GPI-HA. For GPI-HA-induced fusion we have observed examples of a hemifused state as reported previously (Kemble et al., 1994; Melikyan et al., 1995). However, we also frequently observed examples where redistribution of inner leaflet lipids had accompanied movement of outer leaflet lipid, whereas redistribution of the cytoplasmic marker Lucifer Yellow did not occur. The proportion of hemifused complexes decreased with time after the low pH fusion trigger implying that 1) hemifusion is a meta-stable state, even in the case of GPI-HA-mediated fusion and 2) redistribution of both bilayers precedes dilation of an aqueous fusion pore.

Separate monitoring of inner and outer membrane leaflet fusion

We labeled the inner and outer leaflet of resealed ghosts with C_6-NBD-PC and N-Rh-PE, respectively. The different spectral characteristics of the two probes allow easy microscopic discrimination of their spatial distributions. The analogs were chosen to provide a stable asymmetric distribution during and after fusion with HA-expressing cells. Redistribution of N-Rh-PE to the inner leaflet was shown to be negligible as has been previously demonstrated (Connor and Schroit, 1987). We have also shown here that C_6-NBD-PC effectively remains confined to the inner leaflet of ghost membranes as well as the interior of fused WT-HA-expressing CHO cells. This was verified by two independent assays, back-exchange with BSA (van Meer et al., 1987; Kok et al., 1989) and dithionite quenching (McIntyre and Sleight, 1991). A similar assay system has also been developed by Melikyan et al. (1995) using the dye FM 4–64 to report on inner leaflet mixing. This is a readily water-soluble, nonpermeable, double-charged molecule that becomes fluorescent upon partition into membranes. By entrapment of the dye in resealed ghosts the inner leaflet could be labeled (Melikyan et al., 1995). Although in many salient respects our results confirm those of Melikyan et al. (1995) we have observed a wider range of GPI-HA-induced fusion states than they reported. We have shown that this discrepancy is not due to the choice of inner leaflet label (Fig. 8), as a direct comparison between both inner leaflet labels showed them to behave similarly.

Hemifusion in GPI-HA-mediated membrane fusion is meta-stable

In addition to the expected observation of fusion complexes exhibiting exclusive redistribution of the outer leaflet label N-Rh-PE corresponding to the hemifused state, we also observed examples of fusion trigger-dependent inner leaflet redistribution to GPI-HA-expressing cells. These events could be further divided into two classes, restricted fusion (partial redistribution of inner leaflet probe) and full membrane fusion (full redistribution of inner leaflet probe). The percentage of complexes appearing as full membrane fusion increased with time after application of a low pH pulse, whereas the percentage of hemifusion intermediates decreased. Thirty minutes after application of the low pH trigger, all fused complexes had passed beyond the hemifusion stage. The observation of restricted fusion intermediates implies that the transition from hemifusion to a state where inner leaflets mix is reversible or that inner leaflet diffusion is heavily restricted, as the time scale of observation is long relative to the redistribution time for unrestricted probe diffusion (Rubin and Chen, 1990). Under our experimental conditions the hemifused state is meta-stable. In contrast, Melikyan et al. (1995) have reported the hemifused state to be stable. One possible source of this discrepancy is the extent of trypsin cleavage during the course of activation of GPI-HA-expressing cells. We obtained a higher percentage of hemifusion events with milder trypsinization, but the number of observable fusion events also declined, so we did not routinely use this condition. Melikyan et al. (1995) did observe 5–8% of GPI-HA cells labeling with FM 4–64 at 20 min after fusion triggering under conditions where 2% of cells were labeled by aqueous marker. Thus they have observed similar phenomena to those that we report but at a lower incidence.

Formation of intermediates subsequent to inner-inner leaflet mixing requires the transmembrane and/or cytoplasmic domain

Despite commonly observing inner leaflet redistribution, we rarely observed redistribution of the cytoplasmic marker Lucifer Yellow under the same conditions with GPI-HA-expressing cells. Thus, the flux of inner leaflet lipid can be clearly resolved from the dilated fusion pore, in contrast to the tight association between these two properties observed with WT-HA. Progression to a fusion pore permeable to Lucifer Yellow must therefore require the transmembrane or cytoplasmic domain of HA. Theoretical studies by Nanavati et al. (1992) have shown that even a fully lipidic pore can have an energy minimum at a small radius and is not required to enlarge.

Do stages of GPI-HA-mediated membrane fusion resemble intermediates of the WT-HA fusion pore?

The time resolution of our observations does not allow us to resolve whether WT-HA-mediated fusion between CHO cells and erythrocyte ghosts proceeds via a hemifusion intermediate. Tse et al. (1993) reported that a small aqueous pore is formed before the movement of outer leaflet probe,

and recently Blumenthal et al. (1996) have reported similar results. For the hemifusion intermediate to represent a true state relevant to WT-HA before the establishment of a pore it would therefore have to be short-lived and lipid flow temporarily aborted by the transition to the pore state before dilation. The restricted and full membrane fusion states that we have described for GPI-HA-mediated fusion could correspond to a WT-HA fusion intermediate described by Zimmerberg et al. (1994) for which pore conductance surpasses the threshold for lipid flow but the low molecular weight cytoplasmic marker calcein does not move. In this case the transmembrane domain or cytoplasmic tail of HA could be inferred to be required for coalescence of a number of small pores (a specific form of pore dilation). Previous work by Schoch and Blumenthal (1993) has shown that a point mutation in the amino terminus of the HA2 subunit is inhibitory to pore dilation. In one model of the low pH form of HA during the final stages of fusion an interaction between the amino-terminal peptide and the transmembrane domain has been proposed (Guy et al., 1992).

Meta-stability of the hemifusion intermediate

The progression of a lipid stalk to an extended hemifusion diaphragm has been described for fusion of purely lipidic membranes (Chernomordik et al., 1987). However, such a fusion intermediate between biological membranes may be short-lived due to destabilizing factors promoting full fusion (Chernomordik, 1996). For example, packing constraints may increase the energy of the stalk intermediate so that an extended bilayer diaphragm cannot be formed (Siegel, 1993). Melikyan et al. (1995) have proposed that an enlarged hemifusion diaphragm derived from the inner leaflet lipids of each cell requires the exclusion of membrane-anchored fusion proteins. As several HA trimers are believed to form a fusion site (Danieli et al., 1996; Blumenthal et al., 1996), their intermolecular interactions could oppose the development of an extended bilayer diaphragm. Additionally, in fusion of biological membranes mediated by membrane-anchored proteins such as WT-HA or GPI-HA, the proteins themselves may destabilize and/or rupture the hemifusion diaphragm. This might occur in the following ways. First, in the case of WT-HA the mechanical coupling between the ectodomain and the transmembrane domain will oppose establishment of the hemifusion diaphragm or destabilize it (Melikyan et al, 1995). Second, we suggest that a similar argument can also be applied to the amino terminus of HA2, which inserts into the bilayer. It too will be mechanically coupled to the rest of the HA2 subunit. It may simply provide a much less effective disruptor of the transition to the hemifused diaphragm structure, possibly due to the greater flexibility of the extended HA2 ectodomain. In the case of GPI-HA this much weaker mechanical coupling may be a poor but in some cases sufficient substitute for that provided by WT-HA.

We thank Dr. J. M. White, Charlottesville, VA, for the gift of the HA-expressing cells. We are grateful to Dr. T. Pomorski, Berlin, Germany, for the help in inner leaflet labeling ghosts and many helpful discussions. We also thank Dr. O. Gerasimenko, Liverpool, UK, for assistance with the confocal microscope.

REFERENCES

Blumenthal, R., D. P. Sarkar, S. Durell, D. E. Howard, and S. J. Morris. 1996. Dilation of the influenza hemagglutinin fusion pore revealed by the kinetics of individual cell-cell fusion events. *J. Cell Biol.* 135:63–71.

Chernomordik, L. 1996. Non-bilayer lipids and biological fusion intermediates. *Chem. Phys. Lipids.* 81:203–213.

Chernomordik, L. V., G. B. Melikyan, and Y. A. Chizmadzhev. 1987. Biomembrane fusion: a new concept derived from model studies using two interacting planar bilayers. *Biochim. Biophys. Acta.* 906:309–352

Clague, M. J., C. Schoch, and R. Blumenthal. 1993. Toward a dissection of the influenza hemagglutinin-mediated membrane fusion pathway. *In* Viral Fusion Mechanisms. J. Bentz, editor. CRC Press, Boca Raton, FL. 113–132.

Connor, J., and A. J. Schroit. 1987. Determination of lipid asymmetry in human red blood cells by resonance energy transfer. *Biochemistry.* 26:5099–5105.

Connor, J., K. Gillum, and A. J. Schroit. 1990. Maintenance of lipid asymmetry in red blood cells and ghosts: effect of divalent cations and serum albumin on the transbilayer distribution of phosphatidylserine. *Biochim. Biophys. Acta.* 1025:82–86.

Danieli, T., S. L. Pelletier, Y. I. Henis, and J. White. 1996. Membrane fusion mediated by the influenza virus hemagglutinin requires the concerted action of at least three hemagglutinin trimers. *J. Cell Biol.* 133:559–569.

Guy, H. R., Durell, S. R., Schoch, C., and Blumenthal, R. 1992. Analyzing the fusion process of influenza hemagglutinin by mutagenesis and molecular modeling. *Biophys. J.* 62:95–97.

Hanada, K., and R. E. Pagano. 1995. A Chinese hamster ovary cell mutant defective in the non-endocytic uptake of fluorescent analogs of phosphatidylserine: isolation using a cytosol acidification protocol. *J. Cell Biol.* 128:793–804.

Hoekstra, D., T. de Boer, K. Klappe, and J. Wilschut. 1984. Fluorescence method for measuring the kinetics of fusion between biological membranes. *Biochemistry.* 23:5675–5681.

Hughson, F. M. 1995. Molecular mechanisms of protein mediated membrane fusion. *Curr. Biol.* 5:507–513.

Kemble, G. W., T. Danieli, and J. M. White. 1994. Lipid-anchored influenza hemagglutinin promotes hemifusion, not complete fusion. *Cell.* 76:383–391.

Kemble, G. W., Y. I. Henis, and J. M. White. 1993. GPI- and transmembrane-anchored influenza hemagglutinin differ in structure and receptor binding activity. *J. Cell Biol.* 122:1253–1265.

Kobayashi, T., and Y. Arakawa. 1991. Transport of exogenous fluorescent phosphatidylserine analogue to the Golgi apparatus in cultured fibroblasts. *J. Cell Biol.* 113:235–244.

Kok, J. W., S. Eskelinen, K. Hoekstra, and D. Hoekstra. 1989. Salvage of glucosylceramide by recycling after internalization along the pathway of receptor-mediated endocytosis. *Proc. Natl. Acad. Sci. U.S.A.* 86: 9896–9900.

McIntyre, J. C., and R. G. Sleight. 1991. Fluorescence assay for phospholipid membrane asymmetry. *Biochemistry.* 30:11819–11827.

Melikyan, G. B., J. M. White, and F. S. Cohen. 1995. GPI-anchored influenza hemagglutinin induces hemifusion to both red blood cell and planar bilayer membranes. *J. Cell Biol.* 131:679–691.

Morris, S. J., D. P. Sarkar, J. M. White, and R. Blumenthal. 1989. Kinetics of pH-dependent fusion between 3T3 fibroblasts expressing influenza hemagglutinin and red blood cells: measurement by dequenching of fluorescence. *J. Biol. Chem.* 264:3972–3978.

Nüssler, F., B. Schroth, T. Pomorski, A. Herrmann, and M. J. Clague. 1995. Differential mixing of inner and outer membrane leaflets of

erythrocyte ghosts in response to fusion with cells expressing GPI-anchored influenza hemagglutin. *Mol. Biol. Cell.* 6:182a.

Pomorski, T., A. Herrmann, A. Zachowski, P. F. Devaux, and P. Müller. 1994. Rapid determination of the transbilayer distribution of NBD-phospholipids in erythrocyte membranes with dithionite. *Mol. Membr. Biol.* 11:39–44.

Pomorski, T., P. Müller, B. Zimmermann, K. Burger, P. F. Devaux, and A. Herrmann. 1996. Transbilayer movement of fluorescent and spinlabelled phospholipids in the plasma membrane of human fibroblasts: a quantitative approach. *J. Cell Sci.* 109:687–698.

Rubin, J. R., and Y. Chen. 1990. Diffusion and redistribution of lipid-like molecules between membranes in virus-cell and cell-cell fusion systems. *Biophys. J.* 58:1157–1167.

Sarkar, D. P., J. M. Stephen, O. Eidelman, J. Zimmerberg, and R. Blumenthal. 1989. Initial stages of influenza hemagglutinin-induced cell fusion monitored simultaneously by two fluorescent events: cytoplasmic continuity and lipid mixing. *J. Cell Biol.* 109:113–122.

Schoch, C., and R. Blumenthal. 1993. Role of the fusion peptide sequence in initial stages of influenza hemagglutinin-induced cell fusion. *J. Biol. Chem.* 268:9267–9274.

Siegel, D. P. 1993. Energetics of intermediates in membrane fusion: comparison of stalk and inverted micellar intermediate mechanisms. *Biophys. J.* 65:2124–2140.

Tse, F. W., A. Iwata, and W. Almers. 1993. Membrane flux through the pore formed by a fusogenic viral envelope protein during cell fusion. *J. Cell Biol.* 121:543–552.

van Meer, G., E. H. K. Stelzer, R. W. Wijnaendts-Van-Resandt, and K. Simons. 1987. Sorting of sphingolipids in epithelial (Madin-Darby canine kidney) cells. *J. Cell Biol.* 105:1623–1635.

Zimmerberg, J., R. Blumenthal, D. P. Sarkar, M. Curran, and S. J. Morris. 1994. Restricted movement of lipid and aqueous dyes through pores formed by influenza hemagglutinin during cell fusion. *J. Cell Biol.* 127:1885–1894.